Title
Pharmacokinetics, pharmacodynamics and safety studies on URB937, a peripherally restricted fatty acid amide hydrolase inhibitor, in rats

Journal
Journal of Pharmacy and Pharmacology, 71(12)

ISSN
0022-3573

Authors
Vozella, Valentina
Ahmed, Faizy
Choobchian, Paoula
et al.

Publication Date
2019-11-08

DOI
10.1111/jphp.13166

Peer reviewed

JPP JOURNAL OF Pharmacy and Pharmacology
ROYAL PHARMACEUTICAL SOCIETY
JPP Journal of Pharmacy And Pharmacology
Research Paper

Pharmacokinetics, pharmacodynamics and safety studies on URB937, a peripherally restricted fatty acid amide hydrolase inhibitor, in rats

Valentina Vozella[a], Faizy Ahmed[a], Paoula Choobchian[a], Collin B. Merrill[a], Cristina Zibardi[a], Giorgio Tarzia[b], Marco Mor[c], Andrea Duranti[b], Andrea Tontini[b,†], Silvia Rivara[c] and Daniele Piomelli[a,d,e]

[a]Department of Anatomy and Neurobiology, University of California, Irvine, Irvine, CA, USA, [b]Department of Biomolecular Sciences, University of Urbino "Carlo Bo", Urbino, [c]Department of Food and Drug, University of Parma, Parma, Italy, [d]Department of Biological Chemistry and [e]Center for the Study of Cannabis, University of California, Irvine, Irvine, CA, USA

Keywords
analgesia; endocannabinoid; fatty acid amide hydrolase; oleoylethanolamide; URB937

Correspondence
Daniele Piomelli, Department of Anatomy and Neurobiology, University of California, Irvine, 3216 Gillespie NRF, Irvine, CA 92697-4625, USA.
E-mail: piomelli@uci.edu

Received June 27, 2019
Accepted September 1, 2019

doi: 10.1111/jphp.13166

[†]Deceased.

Abstract

Objectives URB937, a peripheral fatty acid amide hydrolase (FAAH) inhibitor, exerts profound analgesic effects in animal models. We examined, in rats, (1) the pharmacokinetic profile of oral URB937; (2) the compound's ability to elevate levels of the representative FAAH substrate, oleoylethanolamide (OEA); and (3) the compound's tolerability after oral administration.

Methods We developed a liquid chromatography/tandem mass spectrometry (LC/MS-MS) method to measure URB937 and used a pre-existing LC/MS-MS assay to quantify OEA. FAAH activity was measured using a radioactive substrate. The tolerability of single or repeated (once daily for 2 weeks) oral administration of supramaximal doses of URB937 (100, 300, 1000 mg/kg) was assessed by monitoring food intake, water intake and body weight, followed by post-mortem evaluation of organ structure.

Key findings URB937 was orally available in male rats (F = 36%), but remained undetectable in brain when administered at doses that maximally inhibit FAAH activity and elevate OEA in plasma and liver. Acute and subchronic treatment with high doses of URB937 was well-tolerated and resulted in FAAH inhibition in brain.

Conclusions Pain remains a major unmet medical need. The favourable pharmacokinetic and pharmacodynamic properties of URB937, along with its tolerability, encourage further development studies on this compound.

Introduction

Nociception is modulated by neurotransmitter systems that operate both in the central nervous system (CNS) and in peripheral organ systems. One prominent example of peripheral control of pain perception is offered by endogenous opioid peptides, which are released from activated immune cells during inflammation and inhibit pain initiation by activating opioid receptors on sensory nerve endings.[1] Substantial evidence indicates that endogenous cannabinoid mediators such as anandamide may serve an analogous function to that of the opioids. Supporting this view, pharmacological activation of peripheral cannabinoid receptors of both CB_1 and CB_2 subtypes inhibits pain-related responses,[2–6] while selective deletion of CB_1 receptor expression in nociceptive neurons of the dorsal root ganglia (DRG) enhances such behaviours.[7] These findings have led to suggest that the peripheral endocannabinoid system may act as a filter for incoming pain signals (for review, see Piomelli and Sasso, 2014).[8]

One way to explore the therapeutic potential of peripheral endocannabinoid-mediated analgesia is to use CNS-impenetrant inhibitors of the anandamide-degrading enzyme, fatty acid amide hydrolase (FAAH).[9–11] Molecules like the O-aryl-carbamate derivative URB937 inhibit FAAH activity outside the brain and spinal cord, from which they are actively extruded by ATP-cassette membrane transporters present in the blood–brain

barrier.[9,11,12] The availability of these probes has allowed researchers to show that blockade of peripheral FAAH activity attenuates nociceptive responses in various animal models of acute and chronic pain, through a mechanism that requires elevation of anandamide levels and subsequent activation of CB_1 receptors outside the CNS.[9,13]

URB937 was the first peripheral FAAH inhibitor to be disclosed[9] and, at the time of this writing, has been used in 25 peer-reviewed articles (PubMed search performed on 13 August 2019). Work in several laboratories has shown that URB937 suppresses pain-related responses in animal models of postoperative and inflammatory pain,[9,13] chemotherapy-induced and diabetes-induced neuropathy[14–16] and migraine headache.[17] Moreover, it attenuates prostaglandin-induced bladder overactivity in rats and improves radiation-induced lung injury in mice.[18] In some models, URB937 has been shown to be significantly more effective and long-lasting than clinically used analgesics, and to be devoid of the adverse events associated with those drugs (e.g. gastric damage, constipation).[13] Importantly, like other FAAH inhibitors, URB937 does not display properties typical of direct-acting cannabinoid receptor agonists (e.g. sedation, motor dysfunction). Thus, the available evidence suggests that peripheral FAAH inhibition may offer a safe and effective approach to pain therapy.

In vivo preclinical studies have shown that URB937 displays a high degree of target selectivity, does not exert genotoxic effects in the Ames' test and does not inhibit the human potassium hERG channel (unpublished results). These findings point to URB937 as a possible candidate for further development. In the present study, we developed a novel LC/MS-MS method for the quantitative analysis of URB937 in tissues and applied this method to the evaluation of the pharmacokinetic (PK) profile and tissue distribution of URB937 after oral administration in male rats. Additionally, we determined the tolerability of single and repeated supramaximal doses of URB937 in rats of both sexes. Neither the PK properties nor the tolerability of URB937 has been fully characterized before. The results suggest that URB937 is orally available and safe for acute and chronic use, thus encouraging efforts to continue its development for the treatment of human pain.

Materials and Methods

Chemicals and solvents

URB937 and URB597 were synthesized at Pharmaron (Tianjin, PR China) using published synthetic methods.[19,20] OEA and [$^2H_4$]-OEA were purchased from Cayman Chemicals (Ann Arbor, MI, USA). Anandamide-[ethanolamine-^{3}H] (20 000 cpm, specific activity 60 Ci/mmol) was from American Radiolabeled Chemicals (St. Louis, MO, USA). LC/MS-grade water, methanol and chloroform were from Honeywell (Muskegon, MI, USA). LC/MS-grade acetonitrile and ammonium acetate were from Sigma-Aldrich (St Louis, MO, USA). Formic acid (FA) was from Thermo Fisher (Houston, TX, USA).

Animals

Adult Sprague Dawley male and female rats (250–300 g) were purchased from Charles River (Wilmington, MA, USA). Upon arrival, the animals were acclimatized to the vivarium in groups of 4 per cage and kept in a temperature-controlled (22 °C) and humidity-controlled environment under a 12 h light/12 h dark cycle (lights on at 6 : 30 A.M.). Animals had free access to standard rodent chow and water. All experiments met the National Institute of Health guidelines for the care and use of laboratory animals (NIH Publications No. 8023, revised 1978) and were approved by the Institutional Animal Care and Use Committee at the University of California, Irvine.

Drug administration

Rats were randomly assigned to vehicle or URB937 administration. URB937 was dissolved in a vehicle consisting of 10% PEG-400, 10% Tween-80 and 80% saline (0.3, 1, 3, 10, 30, 100 mg/kg) for pharmacokinetic/pharmacodynamic (PK/PD) studies or 20% PEG-400, 20% Tween-80 and 60% saline (300, 1000 mg/kg) for toxicity studies. The drug was administered by oral gavage (10 ml/kg) or intravenous injection (1 ml/kg). Stock solutions were prepared immediately before the experiments and were discarded afterwards.

Pharmacokinetic study

Male rats received URB937 (3 mg/kg) by either oral gavage or tail vein injection. The rats were anesthetized and cardiac blood (approximately 5 ml) was collected at the following time points: 0.25, 0.5, 1, 2, 4, 8 h. Alternatively, rats were treated by oral gavage with vehicle or URB937 (0.3, 1, 3, 10, 30, 100 mg/kg) and killed 1 h after treatment. URB937 concentrations were determined in plasma and brain, and PK data were calculated from the time vs plasma concentration profiles. The following PK parameters were calculated using a noncompartmental model: C_{max}, maximal plasma concentration; T_{max}, time at which C_{max} is reached; Cl, clearance; $t_{1/2}$, terminal half-life; V_d, distribution volume; AUC, area under the curve; F%, oral bioavailability.

Acute toxicity study

Vehicle or URB937 (100, 300, 1000 mg/kg) was orally administered once to male and female rats. The animals

were killed and tissues were collected 7 days after administration.

Subchronic toxicity study

Vehicle or URB937 (100, 300, 1000 mg/kg) was orally administered for 14 days to male and female rats. The animals were killed and tissues were collected at the end of the experiment.

Tissue collection

Blood (approximately 5 ml) was collected in anesthetized rats by cardiac puncture and transferred into 4-ml spray-coated K2 EDTA tubes (Vacutainer; BD Bioscience, Franklin Lakes, NJ, USA). Plasma was obtained by centrifugation at 1000*g* at 4 °C for 15 min. Plasma was aliquoted and stored at −80 °C until analyses. Rats were decapitated using a guillotine and livers and brains were collected and immediately frozen on dry ice.

Extraction of URB937 from tissues

Plasma (0.1 ml) or brain tissue (≈50 mg) were transferred into 8 ml glass vials (Thermo Fisher) and proteins were precipitated with ice-cold methanol (0.5 ml) containing URB597 (50 ng/ml). Samples were mixed for 30 s and centrifuged at 2800*g* at 4 °C for 15 min. After centrifugation, the supernatants were loaded onto Captiva-Enhanced Matrix Removal (EMR)-Lipid cartridges (1.0 ml, 40 mg, Agilent Technologies) and eluted applying vacuum (3–5 mmHg). Protein precipitates were suspended in water: acetonitrile (1 : 4, 0.5 ml), mixed for 30 s and centrifuged as described above. The supernatants were collected, transferred onto EMR cartridges, eluted and pooled with the first eluates. Before and after use, the cartridges were washed with water:acetonitrile (1 : 4, 0.2 ml). After the final elution, the vacuum was increased gradually to 10 mmHg to ensure full analyte recovery. Eluates were dried under N_2, reconstituted in methanol (0.1 ml) and transferred to deactivated glass inserts (0.2 ml) placed in amber glass vials (2 ml).

Quantification of URB937

LC/MS-MS analyses were carried out using a 1200 series liquid chromatography system (Agilent Technologies, Santa Clara, CA, USA), consisting of a binary pump, degasser, thermostated autosampler and thermostated column compartment coupled to a 6410B triple quadrupole mass spectrometric detector (Agilent Technologies). The MassHunter software (Agilent Technologies) was used for instrument control, data acquisition and analysis. URB937 was eluted from an Acquity BEH C18 column (1.7 μm, 80 Å, 2.1 × 50 mm) equipped with an Acquity BEH C18 guard column (1.7 μm, 2.1 × 5 mm; Waters Corporation, Milford, MA, USA). Analyses were performed under gradient conditions with a flow rate of 0.5 ml/min. The mobile phase consisted of A: 0.1% formic acid in water and B: 0.1% formic acid in acetonitrile. The column was equilibrated with 20% B, followed by a linear gradient to 89% B in 5.5 min. At 5.51 min the solvent composition was changed to 95% B until stop time at 7 min. Post-time re-equilibration to the original 20% B was done for 5 min. Injection volume was 5 μl with a 1.5 min injection delay time. The column operating temperature was set at 60 °C. The mass spectrometer was operated in the positive electrospray ionization (ESI) mode with drying gas (N_2) temperature set at 300 °C and gas flow set at 12 l/min. Nebulizer pressure was 40 psi. Parent and fragmentation ions for URB937 and URB597 (internal standard, Figure 1a) were determined by separately infusing the analytes (1 μM) into the mass spectrometer, followed by MS-MS scans. Optimization of fragmentation voltage and collision energy were performed to obtain the highest response for the following multiple reaction monitoring (MRM) transitions: *m/z* 355.4 > 230.1 for URB937 and *m/z* 339.4 > 214.0 for URB597 (Table 1). Limit of detection (LOD) was 50 pg/ml and limit of quantification (LOQ) was 300 pg/ml. Under the conditions described above, there was no detectable carry-over of URB937 or URB597 across LC runs. The purity of URB937 and URB597 was tested using the LC protocol outlined above with the MS set in full scan mode and found to be 99.99% and 99.61%, respectively.

Precision, accuracy and recovery

To assess precision, accuracy and recovery, rat plasma (0.1 ml) was spiked with 0.5 ml of methanol containing URB597 (50 ng/ml) and 0.1 ml of URB937 (50, 250 or 1000 ng/ml), and then subjected to EMR fractionation as described above (pre-spiked samples). The dried samples were reconstituted in methanol (0.1 ml) and transferred to deactivated glass inserts (0.2 ml) placed inside amber glass vials (2 ml). A separate set of samples (post-spiked samples) was prepared as follows: plasma proteins were precipitated with methanol (0.6 ml) and the samples were subjected to Captiva EMR-Lipid fractionation. After drying, 0.1 ml of URB937 (50, 250 or 1000 ng/ml) along with 0.5 ml of internal standard solution (URB597, 50 ng/ml) were used to resuspend the samples. The samples were mixed, evaporated under a gentle stream of N_2 and reconstituted in 0.1 ml of methanol. Five replicates of the three concentrations were prepared as pre-spiked and post-spiked EMR matrices and were used to determine precision, accuracy and recovery. Each concentration was run in

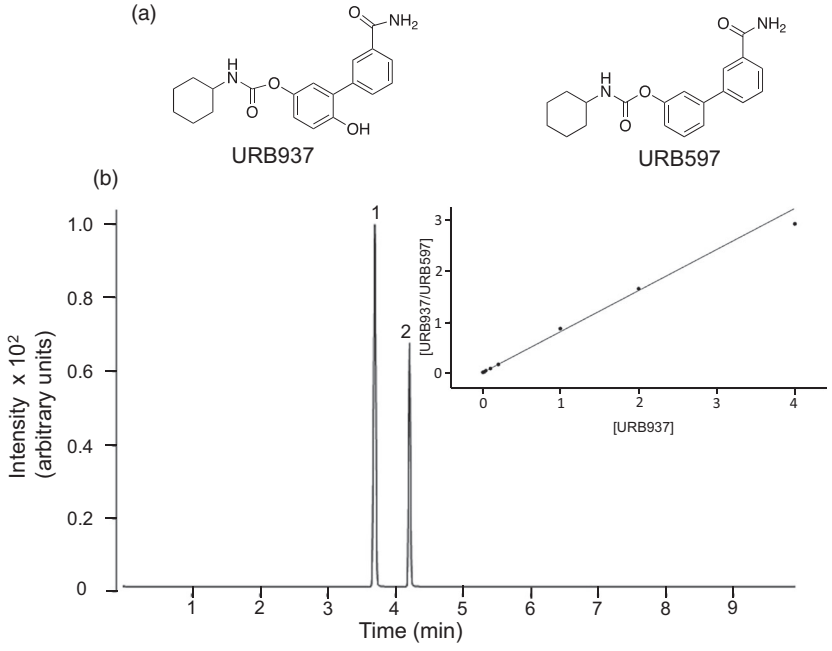

Figure 1 (a) Chemical structures of URB937 and its analogue URB597 (used here as an internal standard). (b) Representative tracing showing the chromatographic separation of URB937 and URB597. Inset: Calibration curve for URB937.

Table 1 Multiple reaction monitoring transitions, optimal fragmentation and collision energies for URB937, URB597 (internal standard), OEA and [$^2H_4$]-OEA

Analyte	Precursor ion (*m/z*)	Product ion (*m/z*)	Fragmentation voltage (V)	Collision energy (V)
URB937	355.4	230.1	150	5
URB597	339.4	214.0	120	20
OEA	326.3	62.1	135	15
[$^2H_4$]-OEA	330.3	66.1	135	15

triplicate on three separate days along with calibration curves in the corresponding matrix, to determine intraday and interday accuracy and precision. Precision was evaluated by calculating per cent relative standard deviation (% RSD) of sample replicates within each day. Accuracy was determined as relative per cent error from nominal concentration and calculated as follows: [(measured value-theoretical value)/(theoretical value)]*100. Extraction recovery was determined as [pre-spiked EMR]/[post-spiked EMR] *100.

Matrix effect

A solution of URB937 (10 μg/ml) in methanol containing 0.1% formic acid was directly infused into the MSD. Infusion was performed with a single syringe pump, through a T-connector that combined the post-column flow with the LC column flow (0.5 ml/min) into the MSD. Infusion rate was 0.3 ml/h and baseline responses were monitored using selected reaction monitoring (SRM) transition for URB937. After steady state was reached, 5.0 μL of pre-EMR (only protein precipitation, without cleanup) and post-EMR plasma matrices were injected into the column, and LC data were collected for each matrix. Pre-EMR plasma showed significant ion suppression around the elution time of URB937 and URB597. However, the suppressing contaminants were completely removed after EMR, as previously shown.[21]

Quantification of OEA

Fatty acid amide hydrolase catalyses the hydrolytic deactivation of multiple amides of long-chain fatty acids with ethanolamine or taurine.[22] The fatty acid ethanolamide (FAE) OEA was selected as a biomarker of FAAH activity, for three main reasons: (1) OEA is significantly more abundant in plasma than other FAEs such as anandamide or palmitoylethanolamide (PEA); (2) OEA is predominantly hydrolysed by FAAH, whereas PEA is predominantly hydrolysed by the cysteine amidase, *N*-acylethanolamine acid amidase (NAAA)[23,24]; and (3) OEA has been previously used as a biomarker for global FAAH inhibition.[25] OEA was extracted from tissues and quantified as previously described.[26] Briefly, plasma (0.1 ml) or frozen rat liver tissue (≈50 mg) was transferred to glass vials and

homogenized in cold methanol (1 ml) containing [$^2H_4$]-OEA (100 pmol). Lipids were extracted with chloroform (2 ml) and washed with LC/MS-grade water (1 ml). After centrifugation at 2850*g* at 4 °C for 15 min, organic phases were collected and transferred to a new set of glass vials. To increase extraction recovery, the aqueous phases were extracted again with chloroform (1 ml) and centrifuged. Organic phases were pooled and dried under N_2. Lipid pellets were reconstituted in chloroform (2 ml) and fractionated by open-bed silica gel column chromatography (Silica Gel G, 60-Å 230–400 mesh; ASTM; Whatman). OEA was eluted with 2 ml of chloroform:methanol (9 : 1, vol/vol). Eluates were collected, evaporated under N_2 and lipids were reconstituted in methanol:chloroform (9 : 1, 0.1 ml). OEA was separated on an Acquity BEH C18 column (1.7 μm, 2.1 × 50 mm, Waters Corporation). The mobile phase consisted of A: 5 mM ammonium acetate with 0.25% acetic acid in water and B: 5 mM ammonium acetate with 0.25% acetic acid in acetonitrile. The flow rate was 0.5 ml/min. The mobile phase conditions were: 85% B from 0 to 2 min, changed to 95% B at 2.01 min and maintained until 4 min (stop time) to remove from the column any strongly retained materials. Equilibration time was 3 min. The total analysis time, including re-equilibration, was 7 min. The column temperature was maintained at 60 °C and the autosampler at 9 °C. The injection volume was 5 μl. To prevent carry-over, the needle was washed in the autosampler port for 30 s before each injection using a wash solution consisting of 10% acetone in water/methanol/isopropanol/acetonitrile (1 : 1 : 1 : 1, by volume). The mass spectrometer was operated in the positive electrospray ionization (ESI) mode, and OEA was quantified by MRM. The capillary voltage was set at 4000 V for all transitions. The source temperature was 300 °C, gas (N_2) flow was 12 l/min and nebulizer pressure was 40 psi. Collision and fragmentation voltages were 15 and 135 V, respectively. OEA-[ethanolamine-^{2}H] ($^2H_4$-OEA) was used as internal standard. Quantifications were performed using the MRM transitions *m/z* 326.3 > 62.1 for OEA and *m/z* 330.3 > 66.1 for [$^2H_4$]-OEA.

FAAH activity

Rat liver and brain were weighed and homogenized in ice-cold Tris-HCl buffer (50 mM, pH 7.5, 1 : 20 weight/volume). Homogenates were centrifuged at 1000*g* for 10 min at 4 °C. Supernatants were collected and protein concentrations were determined using the bicinchoninic acid assay (Pierce, Rockford, IL, USA). To measure FAAH activity, 0.5 ml of Tris-HCl (50 mM, pH 7.5) containing fatty acid-free bovine serum albumin (0.05% weight/volume; Sigma-Aldrich), tissue homogenates (50 μg protein), 10 μM anandamide, and anandamide-[ethanolamine-^{3}H] (20 000 cpm, specific activity 60 Ci/mmol) were incubated at 37 °C for 30 min. The reactions were stopped with chloroform:methanol (1 : 1, 1 ml) and radioactivity was measured in the aqueous layer by liquid scintillation counting.

Food and water intake, body weight

Food and water consumption and body weight (BW) were measured daily for 7 days after single or repeated administration of URB937. Body weight change (% control) was calculated for each animal as follows:

(Body weight at the end of the study
− initial body weight)/initial body weight × 100

Average food and water intake was measured for each cage. The quantities of food provided to and left in each cage were recorded daily throughout the experiment. Food intake per cage was calculated using the total amount of food given to and left in each cage each day before treatment. Food intake (food remained subtracted from food given) was divided by the number of rats in the cage (g/rat/day). From these data the food consumption (in g/100 g BW/day) was determined for each animal. Water consumption was recorded daily by weighing the water bottles when filled and weighing the residues 24 h later. Possible water loss due to spilling was recorded qualitatively based on visual appraisal. The relative drinking water consumption (in ml/100 g BW/day) was determined for each animal.

Blood chemistry

Clinical chemistry measurements were performed at Antech (Fountain Valley, CA, USA) following standard protocols (www.antechdiagnostics.com).

Necropsy and histopathology

Macroscopic abnormalities were assessed post-mortem by visually evaluating the animals' external appearance as well as all shape, colour and weight of all major internal organs. Histopathology analyses were performed at Antech following standard protocols (see above).

Statistics

All results are presented as mean ± SEM. Data were analysed by one-way ANOVA followed by Dunnett's multiple comparison test. Differences between groups were considered statistically significant at values of $P < 0.05$. Statistical analyses were conducted using GraphPad Prism Version 6.01.

Results

Development of a quantitative LC/MS-MS assay for URB937

We developed an LC/MS-MS method for the quantitative analysis of URB937 (Figure 1a) in rodent tissues. Tissue proteins were removed by precipitation with excess cold methanol followed by centrifugation. The close structural analogue of URB937, URB597 (Figure 1a), was added at this step to serve both as carrier and internal standard. The supernatants were eluted through Captiva EMR-Lipid cartridges to remove interfering lipids[21] and the samples were concentrated and subjected to LC/MS-MS analysis. Under the chromatographic conditions described in Materials and Methods, retention times were 3.76 min for URB937 and 4.28 min for URB597, and the total run time was 12 min (Figure 1b). Resolution between analyte and internal standard was >5.5. Peak tailing for both compounds was 1.0–1.2. Retention time and resolution were highly reproducible across chromatographic runs. There was no detectable carry-over across LC runs. Regression analysis of the calibration curve, determined in the absence or presence of matrix applying a $1/x^2$ weighting factor, consistently showed R^2 values >0.99 (Figure 1b, inset). Table 2 shows that interday precision and accuracy were within the ±15% limit set by the United States Food and Drug Administration (https://www.fda.gov/downloads/drugs/guidances). Average extraction recovery ranged from 94.2% to 96.7%.

Table 2 Interday precision, accuracy and extraction recovery of URB937 quantification in plasma matrix

	Day 1	Day 2	Day 3
50 ng/ml			
Measured concentration (ng/ml)	58.54	57.54	56.09
Precision (% RSD)	2.16	2.51	2.25
Accuracy (%)	+17.08	+16.99	+13.39
Recovery (%)	96.14		
250 ng/ml			
Measured concentration (ng/ml)	243.35	242.14	254.88
Precision (% RSD)	3.5	3.87	6.93
Accuracy	−2.66	−3.14	+1.95
Recovery (%)	96.67		
1000 ng/ml			
Measured concentration (ng/ml)	914.5	915.21	950.28
Precision (% RSD)	2.17	1.48	2.78
Accuracy	−8.55	−8.47	−4.97
Recovery (%)	94.17		

Accuracy was measured as [(measured value-theoretical value)/(theoretical value)]*100. Extraction recovery was determined as [pre-spiked EMR]/[post-spiked EMR]*100. N = 5/concentration, each sample run in triplicate.

Pharmacokinetic profile of oral URB937

We applied the protocol outlined above to determine the PK profile of URB937 in male rats after administration of an oral dose (3 mg/kg), which previous studies had shown to fully inhibit peripheral FAAH activity and to exert significant analgesic effects in mice.[13] As shown in Figure 2, URB937 was absorbed at a moderate rate and displayed a peak plasma concentration (C_{max}) of 159.47 ng/ml, which was achieved one hour after administration (Figure 2a). As expected from previous studies,[9,10] the brain levels of URB937 remained below the limit of detection provided by our assay (LOD, 50 pg/ml; LOQ, 300 pg/ml) (Figure 2a,

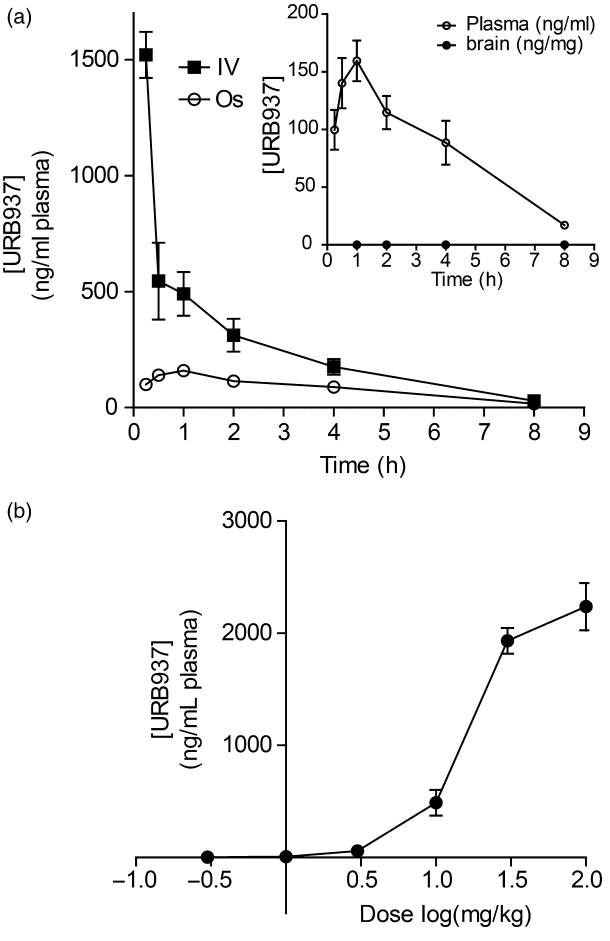

Figure 2 (a) Pharmacokinetic profile of URB937 after single oral (open circles) or intravenous (closed squares) administration (3 mg/kg). Inset: URB937 levels in plasma (open circles) and brain (closed circles) after oral administration. Results are expressed as mean ± SEM (n = 3–4 per group). (b) Dose–response evaluation study. Rats (n = 4 per group) were treated with escalating doses (0.3, 1, 3, 10, 30, 100 mg/kg) of URB937, sacrificed after 1 h and plasma concentrations of the drug were measured by LC/MS-MS. X axis: logarithm of the dose administered.

Table 3 Pharmacokinetic properties of URB937 in male Sprague Dawley rats

	3 mg/kg (oral)
C_{max} [ng/ml]	159.47
T_{max} [min]	60
Cl [ml/min]	76.64
$t_{1/2}$ [min]	162.1
V_d [l]	17.9
AUC_{plasma} [h*ng/ml]	656.2
F [%]	36

AUC, area under the curve; Cl, clearance; C_{max}, maximal plasma concentration; *F*%, oral bioavailability; $t_{1/2}$, terminal half-life; T_{max}, time at which C_{max} is reached; V_d, distribution volume.

inset). The drug was cleared from circulation with a $t_{1/2}$ of approximately 3 h (Table 3). Oral bioavailability was 36%. A dose-escalation study (from 0.3 to 100 mg/kg) showed that plasma levels of URB937 increased linearly in the dose range of 0.3–10 mg/kg and reached saturation between 30 mg/kg and 100 mg/kg (Figure 2b).

Pharmacodynamic profile of oral URB937: FAAH inhibition

In a separate study, we treated rats with ascending doses of URB937 (0.3, 1, 3, 10 mg/kg) and measured FAAH activity in liver and brain homogenates. URB937 inhibited liver FAAH activity with a median effective dose (ED_{50}) of 0.9 mg/kg. Complete inhibition occurred at 3 mg/kg (Figure 3a). By contrast, in brain tissue, URB937 inhibited FAAH activity with an ED_{50} of 20.5 mg/kg, that is, 23 times higher than that observed in the liver.

Pharmacodynamic profile of oral URB937: OEA accumulation

To confirm that URB937 inhibits FAAH in peripheral tissues and identify a possible biomarker for target engagement, we measured levels of OEA in liver and plasma after administration of URB937 (0.3, 1, 3, 10 mg/kg). OEA has been previously used as a biomarker for global FAAH inhibition[25] and offers several practical advantages in this regard over other substrates for this enzyme, including greater abundance in plasma and limited cleavage by other amidases. As shown in Figure 4, URB937 administration was accompanied by a dose-dependent elevation of OEA levels in liver (Figure 4a) and plasma (Figure 4b). A linear regression analysis revealed a strong ($R^2 = 0.90$) linear correlation between liver FAAH inhibition and OEA plasma concentrations in the dose range of 0.3–3 mg/kg (Figure 4c).

Acute and subchronic toxicity studies

We selected three supramaximal oral doses – 100, 300 and 1000 mg/kg – to conduct acute and subchronic toxicity studies. First, to assess acute toxicity, we dosed male and female rats once and monitored them for the following 7 days. Second, to identify potential subchronic toxicity, we dosed male and female rats once daily for 14 days. In both cases, parameters evaluated for treatment-related effects included cumulative food and water intake, body weight, macroscopic examinations at necropsy, blood chemistry, haematology and histopathology. As shown in Figures 5 and 6, regardless of treatment regimen URB937 produced only minor effects, which were not related to the dose administered. In the acute toxicity experiment, male rats treated with the 300 mg/kg dose showed reduced cumulative food and water intake (Figure 5a,c). In the same study, female rats treated with 100 mg/kg displayed a small, but significant increase in food intake (Figure 5b) while female rats treated with 1000 mg/kg showed a larger increment in water consumption (Figure 5d). Subchronic treatment with the 300 mg/kg dose produced a small increase in food intake in female rats (Figure 6b), while minor changes in water intake were observed in animals of both sexes (Figure 6c,d). The body weight trajectory was not affected by any of the doses tested, either after acute

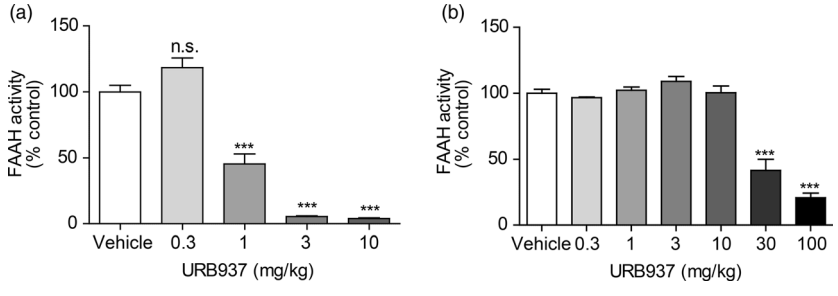

Figure 3 Fatty acid amide hydrolase activity in rat liver (a) and brain (b) one hour after a single oral administration of URB937 (0.3–100 mg/kg). Results are expressed as mean ± SEM (n = 3–4 per group). *$P < 0.05$, **$P < 0.01$, ***$P < 0.001$; one-way ANOVA followed by Dunnett's multiple comparison test.

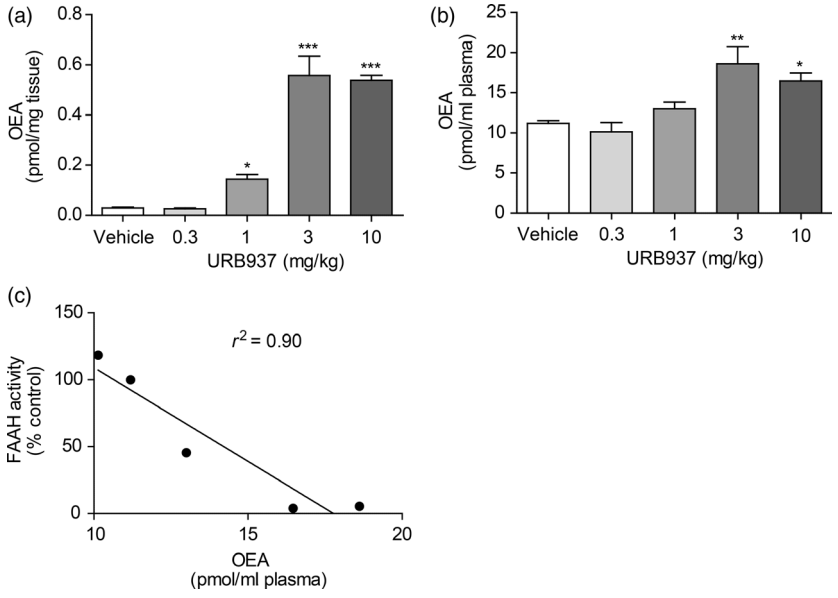

Figure 4 Oleoylethanolamide levels in liver (a) and plasma (b) one hour after a single oral administration of URB937 (0.3–10 mg/kg). Results are expressed as mean ± SEM (n = 4 per group). *P < 0.05, **P < 0.01, ***P < 0.001; one-way ANOVA followed by Dunnett's multiple comparison test. (c) Statistical correlation between oleoylethanolamide levels in plasma and fatty acid amide hydrolase inhibition in liver tissue.

(Figure 5e,f) or subchronic (Figure 6e,f) administration. None of the animals died during the study, and macroscopic examination at necropsy and microscopic histopathology did not reveal any abnormality (representative images from liver tissue are shown in Figure S1). Similarly, no significant alterations were observed in haematology or blood chemistry screens (Tables S1–S8), except for an increase in plasma glucose levels observed only in male rats (Figure 7a). Finally, FAAH activity measurements in brain tissue showed, as expected from prior studies,[9,10] that a substantial level of enzyme inhibition was achieved in CNS with high subchronic dosing (Figure 8).

Discussion

The peripherally restricted FAAH inhibitor URB937[9,11] exerts marked analgesic effects in animal models of acute and chronic pain.[13,14,16,17] In the present study, we developed an accurate and sensitive LC/MS-MS method for the quantification of URB937 in tissues and used this new method to characterize the pharmacokinetic properties of URB937 in male rats. The results confirm that URB937 is orally available and does not enter the CNS at doses that effectively inhibit FAAH activity, elevate peripheral OEA levels, and substantially reduce nociceptive responses.[13] Finally, we found that URB937 is well-tolerated in male and female rats after single or subchronic (2 weeks) administration of supramaximal oral doses (>100 mg/kg).

Establishing a robust analytical assay to measure the concentrations of a drug candidate in biological samples is indispensable to monitor the compound's PK properties during preclinical and clinical studies. The quantitative LC/MS-MS method described here satisfactorily addresses this need. The method was optimized for removal of interfering matrix constituents (achieved by elution through Captiva EMR-Lipid cartridges),[21] speed of chromatographic separation (total run time: 12 min), peak shape (1.0–1.2), resolution between analyte and internal standard (>5.5), reproducibility of retention times across runs, linearity of calibration curves (R^2 > 0.99), interday precision and accuracy (% RSD < 15%) and extraction recovery (94.2–96.7%). The pharmacokinetic profile of oral URB937 in male rats, determined using this method, showed that the compound is orally available (F = 36%), reaches C_{max} one hour after administration and is cleared from circulation with a $t_{1/2}$ of ≈160 min (Figure 2 and Table 2). The relatively short half-life time of URB937 does not negatively impact the pharmacological potency and efficacy of the compound which, like other O-aryl carbamates, inhibits FAAH via covalent attack of the enzyme's catalytic nucleophile.[27,28]

We used the new LC/MS-MS method, combined with measurements of FAAH activity, to determine the tissue distribution of URB937 after oral administration in rats. Confirming previous work,[9,13] we found that the compound is excluded from the CNS (Figures 2 and 3). The mechanism underlying this peripheral segregation has

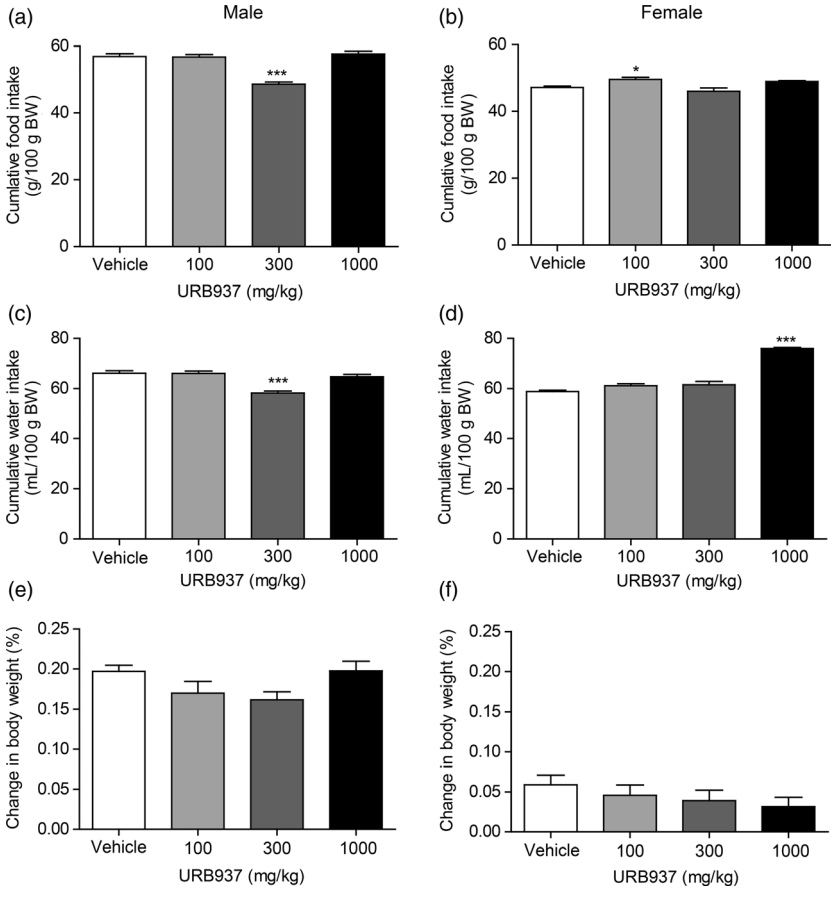

Figure 5 Effects of a single oral dose of URB937 on cumulative food intake in male (a) and female (b) rats. Food intake was measured daily for 7 days after drug administration. Effects of a single oral administration of URB937 on cumulative water intake in male (c) and female (d) rats. Water intake was measured daily for 7 days after drug administration. Effects of a single oral administration of URB937 on body weight (expressed as % change) in male (e) and female (f) rats. Body weight was measured daily for 7 days after drug administration. Results are expressed as mean ± SEM (n = 5 per group). *P < 0.05, **P < 0.01, ***P < 0.001; one-way ANOVA followed by Dunnett's multiple comparison test.

been shown to involve two distinct transmembrane transporters that belong to the ATP-binding cassette family: Abcg2 (breast cancer resistance protein) and Abcb1 (P-glycoprotein).[9,10,12] These transporters are highly expressed in cells of the blood–brain barrier and may act in concert to restrict the access of URB937 to the brain and spinal cord.[12] Supporting this idea, in the present report we confirmed that URB937 does not enter the CNS when administered at therapeutically effective doses (Figures 2a and 3b). The finding that subchronic treatment with high dosages of URB937 (≥100 mg/kg) results in FAAH inhibition in the brain (Figure 8) is also consistent with the existence of a saturable transporter-mediated mechanism of extrusion across the blood–brain barrier. Interestingly, we found that the absorption of URB937 after oral administration reached a plateau between the doses of 30 and 100 mg/kg (Figure 2b), which might also be ascribed to saturation of transporter activity. It is important to point out that our PK and distribution studies were carried out only in male rats, a weakness that will be corrected in future work.

Despite important advances in our basic understanding of nociceptive and inflammatory pain, painful chronic conditions such as diabetic neuropathy, peripheral neuropathy and arthritis remain a pressing medical and socioeconomic problem throughout the world.[29] This problem, which in some countries is further aggravated by an epidemic spread of prescription opiate abuse,[30] calls for the development of new classes of safe and effective analgesic drugs. The endocannabinoid system has emerged as a source for potential analgesic targets due to its pervasive roles in the control of nociceptive processing in the brain, spinal cord and peripheral tissues.[6] In particular, animal studies have demonstrated that the endocannabinoid anandamide modulates pain by activating CB_1 cannabinoid receptors in peripheral nociceptive fibres emanating from DRG

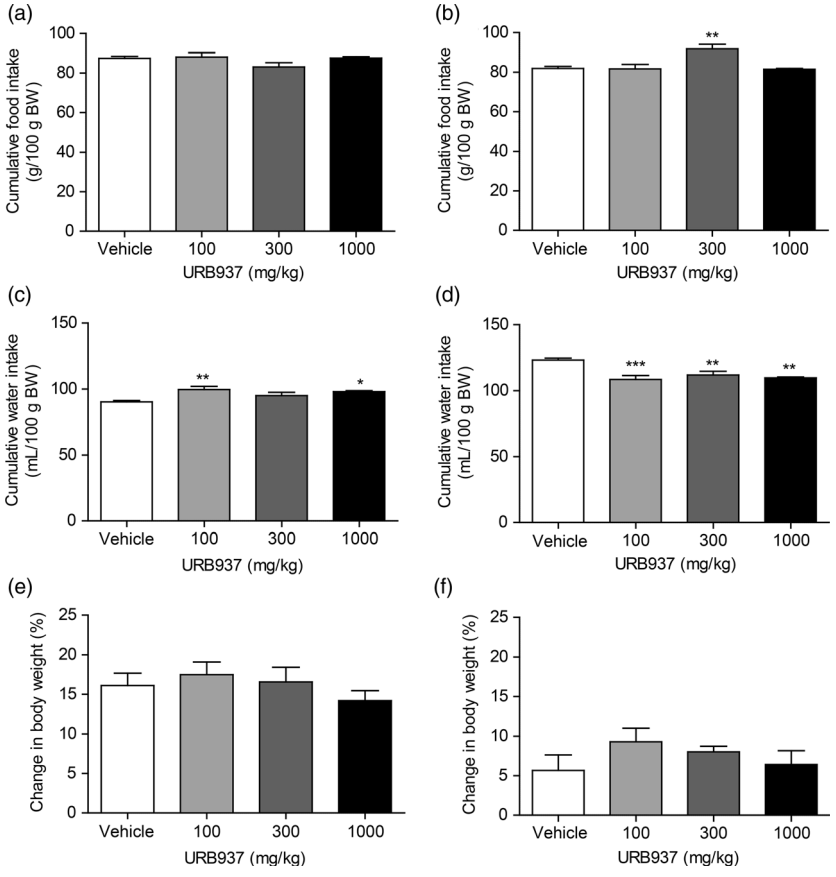

Figure 6 Effects of 14-day administration of URB937 on cumulative food intake in male (a) and female (b) rats. Food intake was measured daily for 14 days after drug administration. Effects of 14-day administration of URB937 on cumulative water intake in male (c) and female (d) rats. Water intake was measured daily for 14 days after drug administration. Effects of 14-day administration of URB937 on body weight (expressed as % change) in male (e) and female (f) rats. Body weight was measured daily for 14 days after drug administration. Results are expressed as mean ± SEM (n = 5 per group). *P < 0.05, **P < 0.01, ***P < 0.001; one-way ANOVA followed by Dunnett's multiple comparison test.

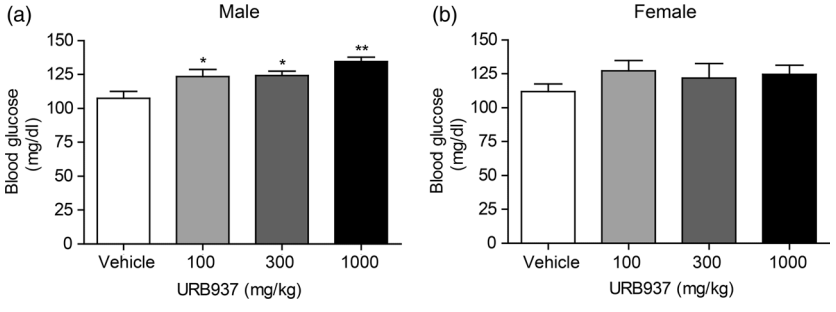

Figure 7 Effect of 14-day administration of URB937 on blood glucose in male (a) and female (b) rats. Results are expressed as mean ± SEM (n = 5 per group). *P < 0.05, **P < 0.01, ***P < 0.001; one-way ANOVA followed by Dunnett's multiple comparison test.

neurons.[2,7,8,31] To explore the biological significance and therapeutic potential of this analgesic mechanism, our lab has developed the first class of potent and selective inhibitors of the anandamide-degrading enzyme, FAAH, which have no access to the brain and spinal cord.[9,11] Despite their lack of CNS penetration, these compounds display marked analgesic properties in rodent models,[9,13–17] suggesting that peripheral FAAH blockade may offer a new approach to pain therapy. This idea is further supported by the low abuse potential associated with FAAH

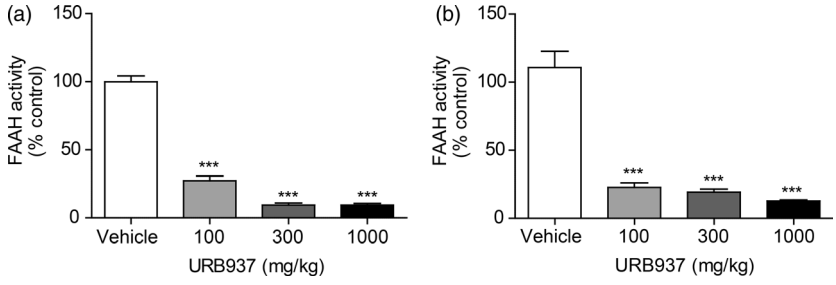

Figure 8 Fatty acid amide hydrolase activity in brain tissue from male (a) and female (b) rats following oral administration of URB937 (100, 300, 1000 mg/kg) for 14 days. Results are expressed as mean ± SEM (n = 5 per group). *P < 0.05, **P < 0.01, ***P < 0.001; one-way ANOVA followed by Dunnett's multiple comparison test.

inhibition[32,33] and by the mild side effect profile reported here for URB937. Our safety studies show, indeed, that URB937 is well-tolerated following acute or subchronic administration in male and female rats, at doses that are >300 times greater than those needed to produce maximal FAAH inhibition in liver and robust analgesia (Figures 5 and 6). Of note, a weakness of these studies, which is currently being addressed in preclinical development work, is that they were not conducted under formal Good Laboratory Practice (GLP) conditions.

Conclusions

The development of safe and effective medicines for pain is a highly urgent medical need. The CNS-impenetrant FAAH inhibitor URB937 displays high analgesic efficacy in animal models of acute and chronic pain and compares favourably in these models with opiates (e.g. morphine) and non-steroidal anti-inflammatory drugs (e.g. indomethacin). The present study investigated the PK profile, tissue distribution and tolerability of oral URB937 in rats. Strengthening previous reports, the findings indicate that URB937 is orally available, peripherally restricted and well-tolerated after acute and chronic oral administration. As such, our results encourage further development of this promising analgesic drug candidate.

Declarations

Conflict of interests

The Authors declare the following conflict of interest: GT, MM, AD and DP are inventors in patents owned by the University of California, Irvine, the Università di Urbino "Carlo Bo", and the Università di Parma, which protect URB937 and its uses.

Acknowledgements

This work was supported by grant R42DA033683-02A1 from the National Institute on Drug Abuse (Principal Investigator, Daniele Piomelli).

References

1. Stein C. New concepts in opioid analgesia. *Expert Opin Investig Drugs* 2018; 27: 765–775.
2. Calignano A *et al.* Control of pain initiation by endogenous cannabinoids. *Nature* 1998; 394: 277–281.
3. Dziadulewicz EK *et al.* Naphthalen-1-yl-(4-pentyloxynaphthalen-1-yl)methanone: a potent, orally bioavailable human CB1/CB2 dual agonist with antihyperalgesic properties and restricted central nervous system penetration. *J Med Chem* 2007; 50: 3851–3856.
4. Anand P *et al.* Targeting CB2 receptors and the endocannabinoid system for the treatment of pain. *Brain Res Rev* 2009; 60: 255–266.
5. Piomelli D *et al.* A lipid gate for the peripheral control of pain. *J Neurosci* 2014; 34: 15184–15191.
6. Woodhams SG *et al.* The cannabinoid system and pain. *Neuropharmacology* 2017; 124: 105–120.
7. Agarwal N *et al.* Cannabinoids mediate analgesia largely via peripheral type 1 cannabinoid receptors in nociceptors. *Nat Neurosci* 2007; 10: 870–879.
8. Piomelli D, Sasso O. Peripheral gating of pain signals by endogenous lipid mediators. *Nat Neurosci* 2014; 17: 164–174.
9. Clapper JR *et al.* Anandamide suppresses pain initiation through a peripheral endocannabinoid mechanism. *Nat Neurosci* 2010; 13: 1265–1270.
10. Moreno-Sanz G *et al.* The ABC membrane transporter ABCG2 prevents access of FAAH inhibitor URB937 to the central nervous system. *Pharmacol Res* 2011; 64: 359–363.
11. Moreno-Sanz G *et al.* Synthesis and structure-activity relationship studies of O-biphenyl-3-yl carbamates as peripherally restricted fatty acid amide hydrolase inhibitors. *J Med Chem* 2013; 56: 5917–5930.
12. Moreno-Sanz G *et al.* Structural determinants of peripheral O-

arylcarbamate FAAH inhibitors render them dual substrates for Abcb1 and Abcg2 and restrict their access to the brain. *Pharmacol Res* 2014; 87: 87–93.
13. Sasso O *et al.* Peripheral FAAH inhibition causes profound antinociception and protects against indomethacin-induced gastric lesions. *Pharmacol Res* 2012; 65: 553–563.
14. Guindon J *et al.* Alterations in endocannabinoid tone following chemotherapy-induced peripheral neuropathy: effects of endocannabinoid deactivation inhibitors targeting fatty-acid amide hydrolase and monoacylglycerol lipase in comparison to reference analgesics following cisplatin treatment. *Pharmacol Res* 2013; 67: 94–109.
15. Sasso O *et al.* Peripheral FAAH and soluble epoxide hydrolase inhibitors are synergistically antinociceptive. *Pharmacol Res* 2015; 97: 7–15.
16. Slivicki RA *et al.* Brain permeant and impermeant inhibitors of fatty-acid amide hydrolase suppress the development and maintenance of paclitaxel-induced neuropathic pain without producing tolerance or physical dependence in vivo and synergize with paclitaxel to reduce tumor. *Pharmacol Res* 2019; 142: 267–282.
17. Greco R *et al.* Effects of peripheral FAAH blockade on NTG-induced hyperalgesia – evaluation of URB937 in an animal model of migraine. *Cephalalgia* 2015; 35: 1065–1076.
18. Li R *et al.* The fatty acid amide hydrolase inhibitor URB937 ameliorates radiation-induced lung injury in a mouse model. *Inflammation* 2017; 40: 1254–1263.
19. Mor M *et al.* Cyclohexylcarbamic acid 3′- or 4′-substituted biphenyl-3-yl esters as fatty acid amide hydrolase inhibitors: synthesis, quantitative structure-activity relationships, and molecular modeling studies. *J Med Chem* 2004; 47: 4998–5008.
20. Fiorelli C *et al.* Development of a multigram synthesis of URB937, a peripherally restricted FAAH inhibitor. *Org Process Res Dev* 2013; 17: 359–367.
21. Vozella V *et al.* Fast and sensitive quantification of Δ 9-tetrahydrocannabinol and its main oxidative metabolites by liquid chromatography/tandem mass spectrometry. *Cannabis Cannabinoid Res* 2019; 4: 110–123.
22. Farrell EK, Merkler DJ. Biosynthesis, degradation and pharmacological importance of the fatty acid amides. *Drug Discov Today* 2008; 13: 558–568.
23. Tsuboi K *et al.* The N-acylethanolamine-hydrolyzing acid amidase (NAAA). *Chem Biodivers* 2007; 4: 1914–1925.
24. Ueda N *et al.* Purification and characterization of an acid amidase selective for N-palmitoylethanolamine, a putative endogenous anti-inflammatory substance. *J Biol Chem* 2001; 276: 35552–35557.
25. Piomelli D *et al.* Pharmacological profile of the selective FAAH inhibitor KDS-4103 (URB597). *CNS Drug Rev* 2006; 12: 21–38.
26. Misto A *et al.* Mast cell-derived histamine regulates liver ketogenesis via oleoylethanolamide signaling. *Cell Metab* 2019; 29: 91–102.e5.
27. Kathuria S *et al.* Modulation of anxiety through blockade of anandamide hydrolysis. *Nat Med* 2003; 9: 76–81.
28. Mileni M *et al.* Crystal structure of fatty acid amide hydrolase bound to the carbamate inhibitor URB597: discovery of a deacylating water molecule and insight into enzyme inactivation. *J Mol Biol* 2010; 400: 743–754.
29. Dahlhamer J *et al.* Prevalence of chronic pain and high-impact chronic pain among adults – United States, 2016. *MMWR Morb Mortal Wkly Rep* 2018; 67: 1001–1006.
30. Volkow ND *et al.* Addressing the opioid crisis globally. *World Psychiatry* 2019; 18: 231–232.
31. Hohmann AG, Herkenham M. Localization of central cannabinoid CB1 receptor messenger RNA in neuronal subpopulations of rat dorsal root ganglia: a double-label in situ hybridization study. *Neuroscience* 1999; 90: 923–931.
32. Gobbi G *et al.* Antidepressant-like activity and modulation of brain monoaminergic transmission by blockade of anandamide hydrolysis. *Proc Natl Acad Sci* 2005; 102: 18620–18625.
33. Justinova Z *et al.* Fatty acid amide hydrolase inhibition heightens anandamide signaling without producing reinforcing effects in primates. *Biol Psychiatry* 2008; 64: 930–937.

Supporting Information

Additional Supporting Information may be found in the online version of this article:

Figure S1. Representative liver sections from male rats treated with vehicle (a) or URB937 (300 mg/kg, daily for 14 days) (b).

Table S1. Effects of a single oral dose of URB937 on complete blood count and differential blood count in male rats.

Table S2. Effects of a single oral dose of URB937 on complete blood count and differential blood count in female rats.

Table S3. Effects of a single oral dose of URB937 on metabolic markers, hepatic function markers, cholesterol, creatine phosphokinase (CPK) in male rats.

Table S4. Effects of a single oral dose of URB937 on metabolic markers, hepatic function markers, cholesterol, creatine phosphokinase (CPK) in female rats.

Table S5. Effects of 14-day administration of URB937 on complete blood count and differential blood count in male rats.

Table S6. Effects of 14-day administration of URB937 on complete blood count and differential blood count in female rats.

Table S7. Effects of 14-day administration of URB937 on metabolic markers, hepatic function markers, cholesterol, creatine phosphokinase (CPK) in male rats.

Table S8. Effects of 14-day administration of URB937 on metabolic markers, hepatic function markers, cholesterol, creatine phosphokinase (CPK) in female rats.